Properties of Interplanetary Coronal Mass Ejections (ICMEs) at 1 AU over the Solar Cycle

L. Jian[1], C. T. Russell[1], and J. G. Luhmann[2]

[1]IGPP and ESS, UC_Los Angeles, [2]Space Sciences Laboratory, UC_Berkeley

Abstract

Herein we present a detailed list of ICMEs at 1 AU for the period 1995-2004 based on Wind and ACE observations. In the course of the study, we find that variation of total perpendicular pressure (Ptpp) is a very effective complementary criterion to distinguish ICMEs from other solar wind disturbances such as stream interactions, and to characterize ICME strength. Of the 227 ICMEs, 67% are associated with shocks. We classify 200 of the ICMEs into 3 groups based on the characteristic temporal variation of Ptpp. Group 1 includes those events that appear to be traversed near the center of the ICME and show evidence for enhanced central magnetic pressure. We find that about 36% are Group 1 events, which is consistent with the conventional wisdom that a magnetic cloud is found during crossings of only one third of the ICMEs. In addition, we examine the variation in the properties of ICMEs over the solar cycle, and find, as expected, characteristic variations in occurrence rate and strength.

Introduction

Interplanetary Coronal Mass Ejections (ICMEs) are the interplanetary manifestations of Coronal Mass Ejections (CMEs), seen in light scattered from enhanced electron densities in the solar corona. The identification of ICMEs is usually based on patterns of change in the individual component of the magnetized plasma: a stronger than ambient magnetic field, a rotating magnetic field, low beta, low ion temperature, declining velocity profile and others. Based on the somewhat subjective criteria, several observers have compiled lists of ICMEs, which are not a little different from each other.

A magnetic field exerts no pressure along its length, but magnetic field and plasma both contribute to the pressure force perpendicular to the field direction. We define total perpendicular pressure, Ptpp, as the sum of the magnetic pressure and thermal pressure ($B^2/2\mu_0$+nkT). If magnetic field lines are straight (no magnetic curvature force), the action of compressional waves should tend to keep Ptpp spatially uniform in the absence of an interaction with an obstacle. If there is a collision of the plasma with an obstacle, a gradient in the pressure will develop that deflects the plasma around the obstacle. In addition, if the magnetic field is twisted and not straight, the magnetic field strength may be higher than if it were straight because twisted magnetic fields can balance pressure gradients. Therefore, Ptpp can assist in the identification of magnetic clouds in ICMEs.

Ideally the identification of stream interactions and ICMEs should be undertaken with the minimum set of parameters necessary for an unambiguous identification. There are many solar wind properties that change during stream interactions and ICMEs, and only a few of these occur sufficiently regularly to be necessary and sufficient identifiers of these two solar wind disturbances. These identifiers are the Ptpp and the solar wind speed. Supplemented with the solar wind flow direction and the magnetic field direction, we have an over determined set of identifiers that can robustly characterize all dynamically active solar wind disturbances.

Signatures in the Total Perpendicular Pressure (Ptpp)

Assuming a constant solar wind electron temperature 130,000 K and a constant 4% fraction of alpha particles by number with a temperature 4 times that of the protons, we have calculated the total perpendicular pressure for all the Wind (SWE and MFI) data and ACE (SWEPAM and magnetometer) data.

In Figure 1, we have inserted a fluxrope as the obstacle to the flow in Spreiter et al.'s [1966] gas dynamic simulation of the flow past a blunt obstacle. The contours show the density which we will take as a rough proxy for the pressure. Depending on where the spacecraft passes through the ICME relative to the center of the flux rope, there are three groups of Ptpp profiles of ICMEs, illustrated by 3 examples of Figures 2-4. For Group 1 ICMEs, the spacecraft penetrates the central fluxrope where magnetic curvature forces (twist in the rope) contribute to enhancing the magnetic field strength and our simple pressure balance calculation is insufficient to describe the forces. Group 2 ICMEs, having a rapid rise (at the shock) with a pressure plateau and a much later return to earlier lower pressure (Figure 3), are interpreted as occurring further from the nose of the obstacle and perhaps the outer parts of the obstacle are penetrated. When the spacecraft just passes through the shock well to one side of the central ICME interaction without entering the magnetic obstacle, we get a pressure profile having a short transient with a rapid rise followed by a decay over hours or over days (Figure 4). These ICMEs are classified as Group 3 ICMEs in our study, and the individual features of the magnetic cloud, such as the stronger than ambient and rotating magnetic field, may not be recognizable. Here the behavior of Ptpp assists our identification.

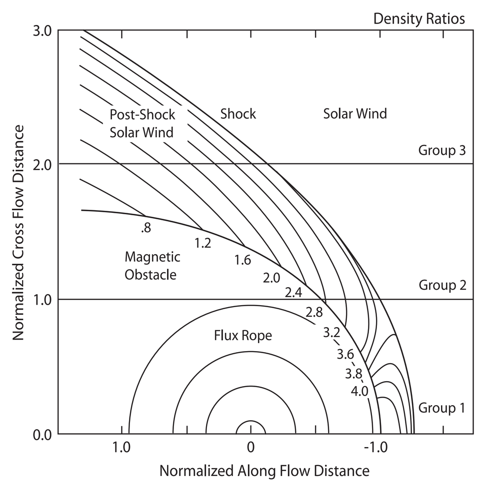

Figure 1. Interpretive sketch of ICME encounters using Spreiter et al. (1966) gasdynamic simulation results. Group 1 events encounter the magnetic flux rope. Group 2 events encounter the ICME near the obstacle. Group 3 events catch the shock away from the obstacle.

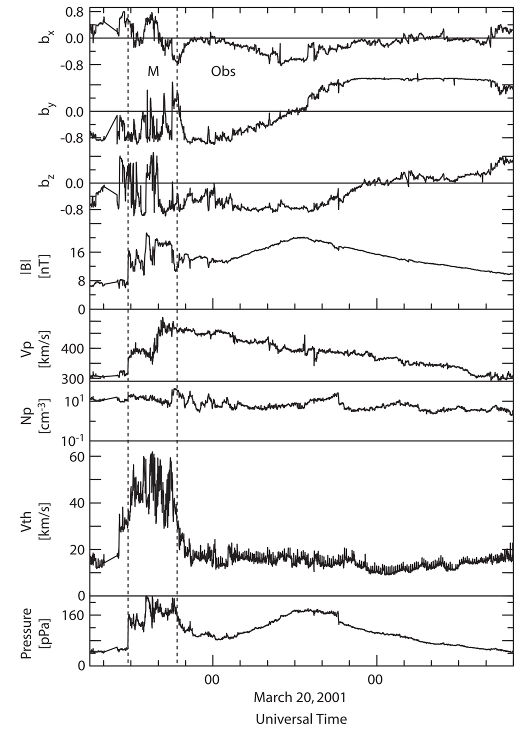

Figure 2. Group 1 ICME

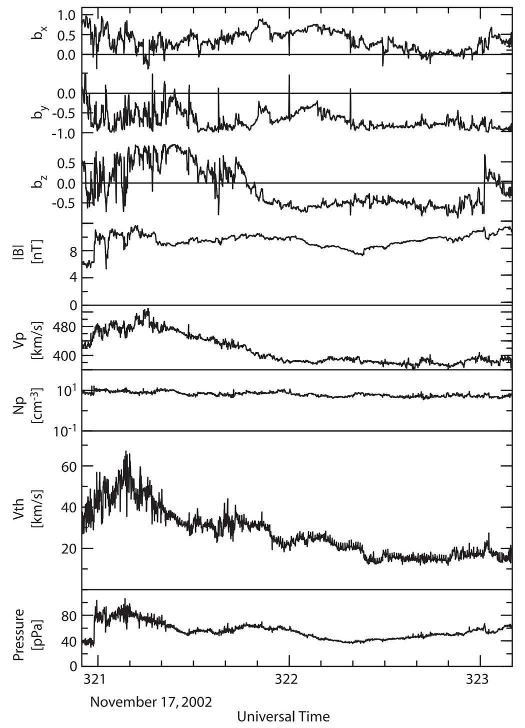

Figure 3. Group 2 ICME.

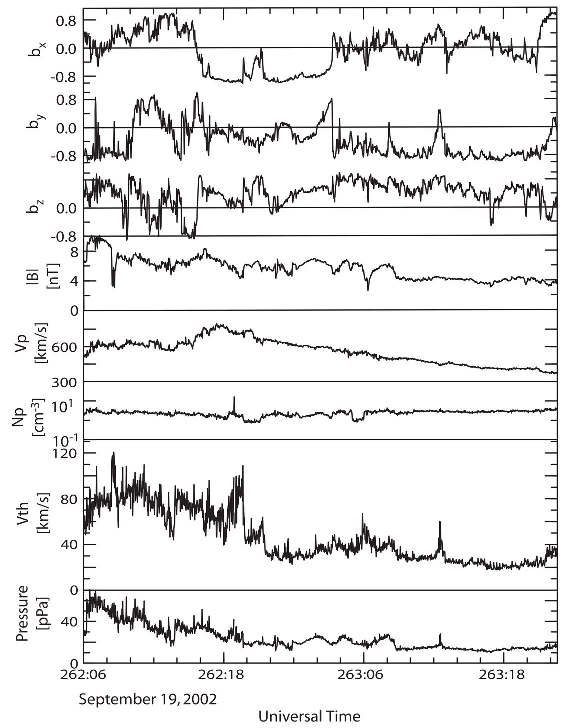

Figure 4. Group 3 ICME.

Table 1. A Sample of the List of ICMEs

#	Start UT	End UT	Duration [hr]	Discontinuity UT	F/R Shock	ΔP [pPa]		Pmax [pPa]	Vmax [km/s]	Vmin [km/s]	ΔV [km/s]	Bmax [nT]	Group	C+R	Lepping	Comments	MC
								2002									
1	02/28 0200	03/04 0000	94.00	02/28 0507	F	50 -> 240	190	140	440	325	-115	14.6	1	1	N	V irregular	0
2	03/19 0620	03/20 1200	29.67	03/18 1315	F	50 -> 350	300	213 (600)	450 (480)	320	-130	22.5	3	2	2	T is not low	1
3	03/20 1200	03/22 0300	39.00	03/20 1320	/	80 -> 188	108	350	616	415	-201	21	1	0	N		0
4 *	03/24 1200	03/25 2100	33.00	03/23 1125	F	22 -> 81	59	180	490 (520)	410	-80	21	1	2	2	V irregular, followed by a SIR	2
				03/25 0115	F	105 -> 180	75										
5	04/14 1100	04/15 1800	31.00	04/14 1149	F	43 -> 73	30	90	440	332	-108	11	3	N	N	ACE, BDE	0
6	04/17 2035	04/19 0825	35.83	04/17 1102	F	100 -> 800	700	100 (900)	640	430	-210	14.5 (33)	3	1	1	followed by another shock	1
7	04/20 0045	04/21 1630	39.75	04/19 0827	F	50 -> 235	185	200 (265)	650	440	-210	21.5 (23.7)	1	2	3		1
8	04/23 0400	04/24 1700	36.00	04/23 0415	F	40 -> 275	235	310	650	472	-198	17	3	N	N	ACE, Tp high	0
9	05/10 1100	05/11 1000	23.00	05/10 1114	/	40 -> 110	70	180	418	330	-88	15.5	3	N	N		0
10 *	05/11 1000	05/12 1400	28.00	05/11 1030	F	60 -> 270	210	320	470	400	-70	17.5 (23)	2	N	N	ICME (05/11 1618~05/12 0100, T not low) + SIR	
				05/12 0234	R	48 -> 24	-24										
11	05/19 0240	05/20 0257	24.28	05/18 1920	F	37 -> 270	233	208 (370)	475 (500)	380	-95	20	3	N	1	ACE	0
12	05/20 0300	05/21 2100	42.00	05/20 0335	/	38 -> 103	65	148	533	370	-163	16	3	0	N		0
13	05/23 1000	05/25 1600	54.00	05/23 1016	F	150 -> 550	400	1400	975	360	-615	54	3	2	3	ACE, strong, BDE	1
14	07/17 1500	07/19 0730	40.50	07/17 1526	F	50 -> 300	250	260	540	408	-132	19.5	3	0	N	ACE, BDE	0
15 *	07/19 0930	07/22 0450	67.33	07/19 0932	F	18 -> 85	67	200	925	480	445	20	1	0	N	good SIR+ICME, ACE, BDE, big deflections of V	0
				07/19 1443	F	50 -> 110	60										
16	07/25 1300	07/27 0610	41.17	07/25 1300	F	40 -> 85	45	100	550	400	-150	13.8	3	N	N	ACE, T not low, BDE	0
17	08/01 0425	08/01 2220	17.92	08/01 0425	F	30 -> 100	70	120	463	430	-33	15	1	2	3	ACE, followed by another ICME	1
18	08/01 2220	08/03 0526	31.10	08/01 2220	F	45 -> 125	80	130	525	407	-118	16	1	0	2	ACE	0
19	08/19 0842	08/21 2115	60.55	08/18 1810	F	13 -> 140	127	90 (200)	520 (600)	370	-150	12.5 (16.7)	3	1	N	ACE	0
20	08/26 1030	08/26 2300	12.50	08/26 1115	F	50 -> 160	110	230	430	355	-75	17	3	N	N		0
21 *	09/08 0413	09/08 2000	15.78	09/07 1622	F	30 -> 250	220	193 (290)	505 (620)	450	-55	12.3 (23)	3	0	N	ICME + ICME	0
22 *	09/08 2045	09/10 2000	47.25					60	552	385	-167	10	2	0	N		0
23	09/19 0600	09/20 2235	40.58	09/19 0616	F	30 -> 60	30	90	780	370	-410	10.2	3	0	N		0
24 *	09/30 2200	10/01 1430	16.50	09/30 0755	F	140 -> 360	220	300	430	350	80	26.5	1	2	3	ICME in SIR	0
25	10/02 2200	10/04 2200	48.00	10/02 2241	F	14 -> 36	22	100	543	370	-173	14	2	2	N		0
26	11/17 0722	11/18 2346	40.40	11/16 2305	/	37 -> 67	30	70 (90)	480 (510)	380	-100	11.3	2	2	N	ACE, bad	0
27	11/26 2000	11/29 0700	59.00	11/26 2110	F	60 -> 440	380	510	600	480	-120	29	3	N	N	ACE, Pmax ~770 based on WIND data	0

F/R shock: forward/reverse shock; *: Hybrid events; /: not a shock; N: not in the list; ( ): values in the sheath region; BDE: bidirectional solar wind electron strahls from ACE.
C+R: Cane, H.V., and I.G. Richardson, Interplanetary coronal mass ejections in the near-Earth solar wind during 1996-2002, *J. Geophys. Res.*, 108, 1156, 2003; and also from personal communication.
Lepping MC (magnetic cloud) list is available from http://lepmfi.gsfc.nasa.gov/mfi/mag_cloud_pub1.html, and 2004 data are not available

Table 2. Comparison of ICMEs in 3 Groups and with Other Lists

Year	ICME						Total ICME # in the 3 Groups	ICME #	C+R ICMEs #	C+R MCs #	Lepping MCs #
	Group 1		Group 2		Group 3						
	#	%	#	%	#	%					
1995	4	36.36	5	45.45	2	18.18	11	11	NA	NA	8
1996	5	71.43	1	14.29	1	14.29	7	7	4	4	4
1997	10	50.00	4	20.00	6	30.00	20	20	22	14	17
1998	7	38.89	3	16.67	8	44.44	18	24	37	10	11
1999	6	37.50	3	18.75	7	43.75	16	22	33	3	4
2000	16	45.71	3	8.57	16	45.71	35	37	54	9	14
2001	7	23.33	2	6.67	21	70.00	30	38	48	7	10
2002	8	29.63	4	14.81	15	55.56	27	27	26	10	10
2003	6	31.58	6	31.58	7	36.84	19	22	22	5	4
2004	3	17.65	5	29.41	9	52.94	17	19	20	6	NA
All	**72**	**36.00**	**36**	**18.00**	**92**	**46.00**	**200**	**227**	**266**	**68**	**82**

Table 3. ICME Statistics

Year	ICME #	# with Shock	% with Shock	<Pmax> (δ Pmax)	<Bmax> (δ Bmax)	< R=Vmax/Vmin > (δ R)	< ΔV > (δ ΔV)
1995	11	5	45.5	112.73 (30.45)	13.34 (1.65)	1.22 (0.04)	64.73 (15.03)
1996	7	1	14.3	101.43 (19.29)	11.24 (1.33)	1.27 (0.04)	92.86 (16.54)
1997	20	9	45.0	158.90 (20.54)	15.55 (1.22)	1.31 (0.03)	73.20 (21.76)
1998	24	17	70.8	230.63 (44.19)	18.06 (1.64)	1.35 (0.03)	127.54 (22.93)
1999	22	14	63.6	173.77 (34.80)	16.16 (1.70)	1.46 (0.09)	75.45 (44.48)
2000	37	28	75.7	233.20 (60.20)	16.87 (1.38)	1.28 (0.03)	117.29 (12.72)
2001	38	27	71.1	253.39 (61.57)	19.88 (2.20)	1.41 (0.03)	143.22 (23.07)
2002	27	22	81.5	233.04 (49.09)	18.27 (1.65)	1.42 (0.06)	127.44 (32.57)
2003	22	16	72.7	271.81 (66.59)	20.18 (2.62)	1.45 (0.05)	206.90 (32.32)
2004	19	13	68.4	179.00 (36.09)	17.65 (2.00)	1.29 (0.03)	136.21 (16.04)
All	**227**	**152**	**67.0**	**212.48 (17.76)**	**17.49 (0.63)**	**1.36 (0.02)**	**122.44 (8.88)**
Max	**38**	**28**	**81.5**	**2250**	**72**	**2.96**	**615**
Min	**7**	**1**	**14.3**	**20**	**3.5**	**1.06**	**30**

Table 4. Hybrid Events

Year	1995	1996	1997	1998	1999	2000	2001	2002	2003	2004	All
Hybrid #	6	3	5	12	9	14	9	10	4	7	79
ICME + ICME	1			5	2	3	4	1			**16**
ICME + SIR	2	2	1	2	3	2	1	2	3	4	**22**
ICME with SIR				1	1	3	1	1	1		**8**
SIR + ICME			1	3	2	5	1	2		2	**16**
ICME in SIR	3	1	3	1		1	2	4		1	**16**
ICME + SIR + ICME					1						**1**

Figure 5. Annual Statistics of Some Properties of ICMEs

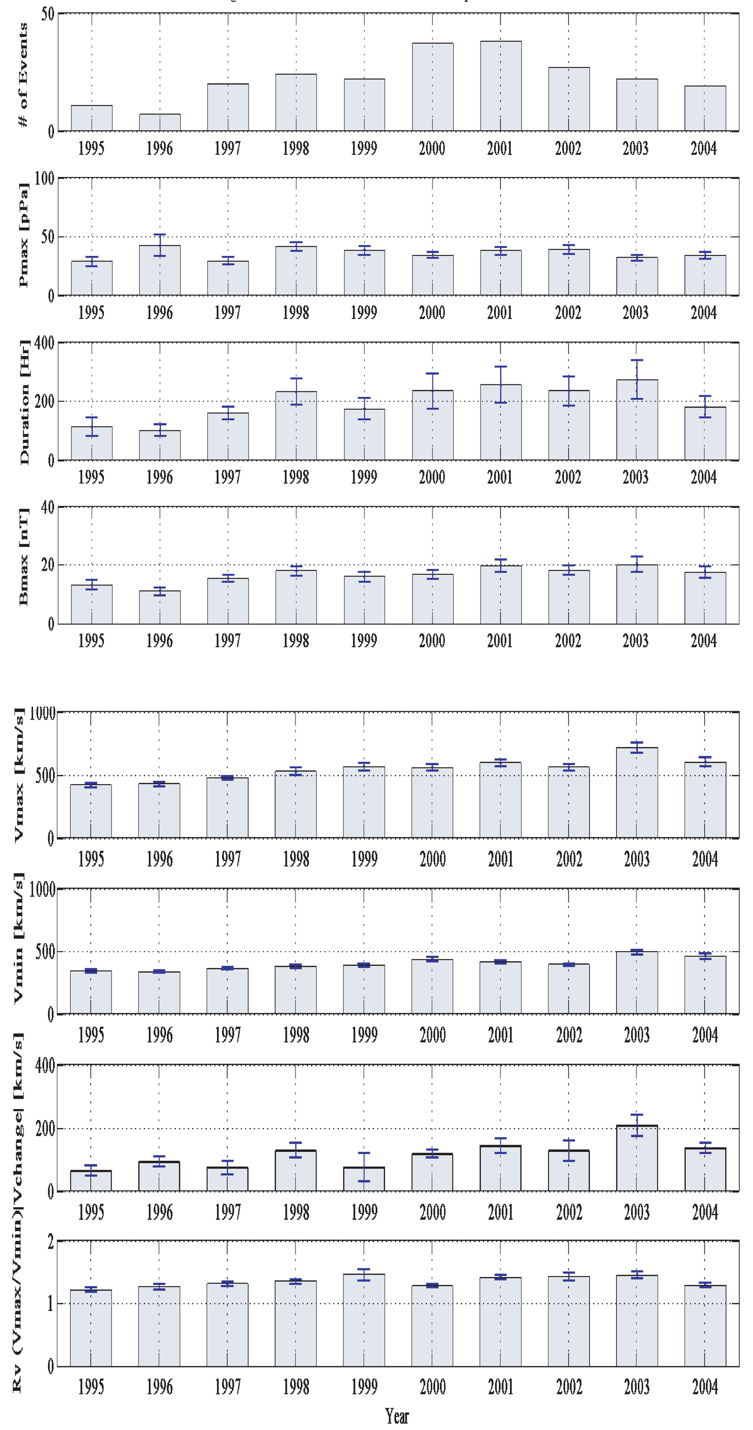

Figure 6. Probability Distribution: Pmax of ICMEs (1995~2004)

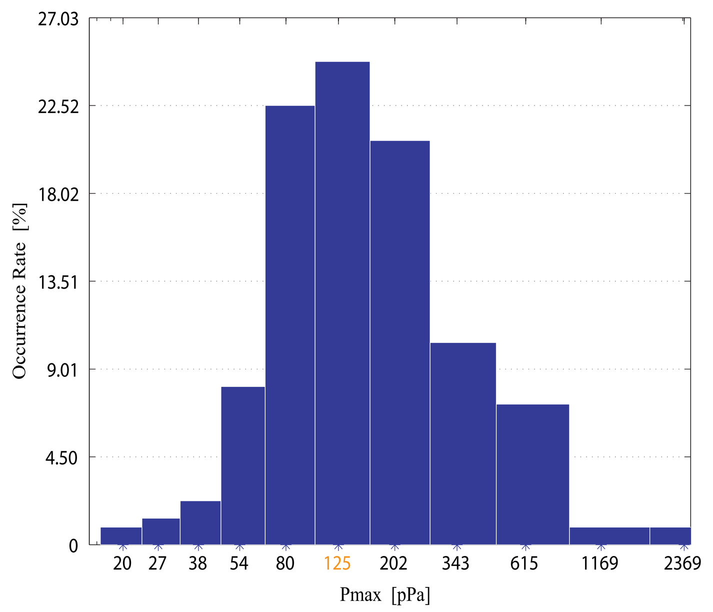

Variation of the Properties of ICMEs during the Period 1995-2004

Mainly depending on the behavior of the total perpendicular pressure (Ptpp) and also considering the individual criterion of ICMEs, but not confined to magnetic clouds, we have classified 227 ICME events from 1995-2004 Wind and 1998-2004 ACE solar wind data. So, the annual average ICME event number is about 23. Based on two spacecraft, we feel more confident than before, but we do not rule out that we might miss some events due to data gaps and noise.

We denote ΔP as the change of the Ptpp across the discontinuity, Pmax, Bmax as the peaks of Ptpp and B, Rv as the ratio of Vmax to Vmin, ΔV as the change in the solar Wind speed during each event. In the study, we define the boundary between which we can see the apparent flux rope structure and properties, rather than starting from the magnetic sheath region. However, if there is no obvious magnetic obstacle boundary, we fix the boundary at the jump of pressure if there is a shock; if neither, we generally set the boundary based on the behavior of total pressure, like where the pressure structure emerges from and decays back to the ambient solar Wind.

Table 1 presents a detailed list of ICMEs for 2002. And similarly we list ICME events for the whole 10 years. For a discontinuity simply indicated by Ptpp, we basically check the V, Np, Tp, B one by one, to verify if it is a forward or reverse shock. From the list, we emphasize that most ICMEs have the declining solar wind velocity, indicated by the negative value of ΔV.

We classify 200 ICMEs with clear characteristics in Ptpp into 3 groups, shown in Table 2. And among them, there are 72 Group 1 events, indicating that about 36% of ICMEs are encountered by the Wind or ACE through the flux rope. This is consistent with the general wisdom that about 1/3 ICME observations are encounters with magnetic clouds. This suggests in turn that all ICMEs may contain magnetic clouds but the spacecraft does not pass through this cloud in the majority of the events. In Table 2, we also list the number of our identified ICMEs and compare them with ICMEs identified by Cane and Richardson (not confined to magnetic clouds, MCs, and confined to MCs) as well as MCs identified by Lepping for the 10 years. Generally, we find over 10 fewer events per year than Cane and Richardson during 1998-2001. However, as expected, the number of Group 1 events in each year is close to the count of MCs by the other two groups.

Table 3 lists the number of ICME events, the number and percentage of eventsmean for the 10 years, also the maximum and minimum values among all events during the 10 years. In all, 67.0% of ICMEs occur with shocks. We have found no ICMEs associated with forward-reverse shock pairs. This number is 2.20% of all ICMEs. Additionally, Figure 5 shows the solar cycle variation of the annual ICME statistics. Besides the parameters in Table 3, Figure 5 also displays the variation of Duration, Vmax, Vmin of events. Averaged over all these events, Pmax is 212±18 pPa; Bmax is 17.5± 0.6 nT; Rv is 1.36±0.02, and ΔV is -122±9 km/s, where the uncertainty is the probable error of the mean.

In contrast to SIRs, the occurrence rate of ICMEs has a clear solar cycle dependence, with a maximum occurrence of 38 events in 2000, at solar activity maximum, and a minimum occurrence of 7 events in 1996, at solar minimum. The duration and change in velocity of events are both generally larger around solar maximum than solar minimum. In addition, the Pmax distribution is quite wide, centered on 125 pPa, varying from 20 pPa up to 2250 pPa, as illustrated in Figure 6.

Moreover, there are 79 hybrid events over the 10 years, and we list them in Table 4. Such events consisting of more than 1 event are usually more geoeffective and may lead to better understanding of the heliospheric structure near the Sun.

Conclusions

Total perpendicular pressure Ptpp has a simple temporal variation, smooth except for shocks, while the temporal variations of its individual components are not simple. Depending on the position of the spacecraft passing through the ICME, we can classify the Ptpp of ICMEs into three groups. Corresponding to Group 1, 2 and 3 ICMEs, the profile of Ptpp has a central pressure maximum, a sharp rise followed by a steady plateau, and a gradual decay respectively. From 1995-2004 the solar wind data from Wind and ACE, we identify 227 ICMEs, and 67% of these ICMEs occur with forward shocks. The occurrence rate and change in velocity of ICMEs both have a clear solar cycle dependence. The peak pressure Pmax has a broad distribution, centered on 125 pPa, with the average value 212±18 pPa. We also classify 79 interesting hybrid events.

We look forward to the launch of STEREO that will allow us to make two to three (using ACE or WIND) cuts through ICMEs at varying distances from the center, enabling us to establish the ecliptic longitude variation of these structures and to test our hypothesis that the pressure signature of ICMEs depends on the impact parameter.

Acknowledgements

This work is supported by the IGPP branch at LANL. We have used the Wind plasma and magnetic field data throughout. We thank the MIT and Goddard plasma team (A.J. Lazarus and K. Ogilvie) and the magnetometer team (R.P. Lepping) for making these data available. We have supplemented this study with ACE data. We thank the PI of the plasma analyzer (D. McComas) and the magnetometer PI (C.W. Smith) for making these data publicly available, and also thank J. Steinberg and R. Skoug for giving us the access to ACE STEA electron pitch angle plots.